

In situ study of the dewetting behavior of Ni-films on oxidized Si(001) by GISAXS

R. Felici^{a,*}, N.M. Jeutter^a, V. Mussi^b, F. Buatier de Mongeot^b, C. Boragno^b, U. Valbusa^b, A. Toma^b, Y. Wei Zhang^c, C. Rau^c, I.K. Robinson^d

^a *E.S.R.F., 6 Rue Jules Horowitz, 38043 Grenoble, France*

^b *Dipartimento di Fisica, Università di Genova, via Dodecaneso, 16146 Genova, Italy*

^c *Department of Physics, University of Illinois at Urbana-Champaign, 1110 West Green Street, Urbana, IL 61801-3080, USA*

^d *University College London, 20 Gordon Street, London WC1H 0AJ, UK*

Available online 29 April 2007

Abstract

Metal nano clusters are of great importance in physical and chemical science. One simple method for obtaining metal clusters consists in the deposition of a metal film on an inert substrate followed by annealing at high temperature. After this procedure, the metal film reduces in small clusters, whose morphology depends on the annealing temperature and annealing time. In this work we present a grazing incidence small angle X-ray scattering (GISAXS) study carried out in situ to understand the nucleation and formation of Ni metal clusters. For this purpose uniform Ni metal films, of different thicknesses, were deposited onto an oxidized Si(001) substrate, and annealed at different temperatures in the range 400–800 K. Before annealing the samples were characterized by X-ray reflectivity measurements to exactly determine the values of the thickness and of the starting roughness. The GISAXS patterns show a surface roughness increase starting at about 600 K. By increasing the temperature the diffused intensity breaks in two lines around the reflectivity plane, indication of a characteristic length correlation of the roughness. This correlation length is maintained during the metal clusters formation.

© 2007 Elsevier B.V. All rights reserved.

Keywords: Metal clusters; Dewetting; GISAXS; X-ray reflectivity; Nickel; Silicon oxide; Silicon

1. Introduction

Clusters, grown on inert substrates, are an important subject for modern technology. They are the basis for the development of new devices, as memory arrays [1,2], and they are also used as catalysts for the growth of semiconducting nanowires [3] or carbon nanotubes [4,5]. Moreover they are also studied as a model system to better understand the role of the metal catalyst in heterogeneous gas reactions [6].

A common, simple and widely applied method for the production of metal clusters with nanometric dimensions is based on the dewetting of a thin film deposited on an inert substrate. This is a self-agglomeration process induced

by annealing at high temperature [7]. This process has the advantage of being easy to be introduced in any growth procedure, however it results in the production of metal islands with a broad distribution of sizes and spacings. An attempt to overcome this limitation is based on the use of nano-patterned substrates. In this case the dewetting process results in metal clusters following the substrate template and they show a more defined size distribution as well as an ordering along a preferred crystallographic direction [8].

Even if the process of metastable thin solid film dewetting has been known for a long time, it is still of interest from a fundamental point of view because the leading forces of the process have not been fully understood. In general terms dewetting of a metastable liquid film can occur through two different mechanisms which depend on the spreading coefficient of the material onto the particular

* Corresponding author.

E-mail address: felici@esrf.fr (R. Felici).

substrate [9]: (a) in the case of a thin non-wetting film, the system is unstable against spinodal decomposition, induced by thermally activated capillary waves at the free surfaces, and breaks into microscopic droplets with a size depending on the square of the thickness; (b) in the case of a thin wetting layer the dewetting process can still occur and it is activated by nucleation and growth of dry spots, which, in the case of thin polycrystalline films, can occur at grain boundaries [10]. In this case the average dimension of the islands scales linearly with the thickness. In the case of solid metal films, dewetting occurs, but many details on the process leading to the formation of the clusters are still unknown. Some authors report that the spinodal decomposition is the driving force, while others tend to prefer the grooving process occurring at grain boundaries.

Many morphological studies are present in the literature dealing with the surface morphology of the final state [11] but only few have been carried out in real-time to understand the dynamics of the film breaking [12]. Grazing incidence small angle scattering (GISAXS) is a technique, able to determine the morphology and the correlation of small clusters at the surface [13] and it has also been used to study in situ the time evolution of surface nanostructures [14]. In this article, we report first results of GISAXS experiments carried out in situ during the dewetting process of thin Ni-films with different thicknesses deposited on amorphous SiO₂ substrates.

2. Experimental

The GISAXS experiments have been carried out on the UniCAT 34-Sector C Beamline of the Advanced Photon Source (APS), Chicago (USA). This beamline, which was conceived to carry out coherent X-ray scattering experiment, is an in-vacuum beamline equipped with a small UHV chamber. The beamline design allows the X-ray beam to reach the sample without crossing any Be window. This is of particular advantage when it is necessary to measure a small X-ray scattering signal due to the presence of nano clusters, whose scattering intensity is comparable with the diffuse scattering of any Be window. For this experiment we used a photon energy of 8 keV and a beam size of 100 × 50 μm as determined by the slits placed 15 cm before the sample position.

The UHV chamber has a base pressure of 10⁻⁹ Torr and it is equipped with an Oxford Instrument e-beam evaporator. The films were deposited in situ onto Si(001) substrates covered by a 30 μm thick amorphous silicon oxide layer. The evaporation of Nickel was controlled by monitoring the deposition time while keeping the power of the evaporator constant to 25 W. Before opening the shutter the evaporator was slowly brought to the nominal power and kept for few minutes at the deposition condition. During the deposition the substrate was kept at 400 K, temperature resulting in the production of films with a small surface roughness. The temperature was measured using a thermocouple attached to one of the tantalum clips hold-

ing the sample on the boraelectric heater. The thickness of the Ni-film was determined by X-ray specular reflectivity measurements. The data were fitted using the Parratt32 reflectivity tool from the HMI Institut in Berlin [15].

The GISAXS pattern was recorded using a Princeton CCD camera placed on the diffractometer arm. The calibration of the CCD camera leads to a pixel to angle conversion of 0.00182° per pixel corresponding to an exchange wavevector resolution of 1.27 × 10⁻⁴ Å⁻¹ on both directions, perpendicular and parallel to the surface. The GISAXS measurements were carried out using an X-ray angle of incidence of 1° and recording with the CCD camera the diffused intensity with an exit angle between 0° and 0.8°. The typical acquisition time for each image was 30 s.

3. Results

One of the parameter necessary to understand the dewetting process is the thickness of the metal film. For this reason before starting the annealing of the samples, we have measured the X-ray specular reflectivity intensity as a function of the exchanged vertical momentum. In Fig. 1, we show the experimental data from three samples deposited

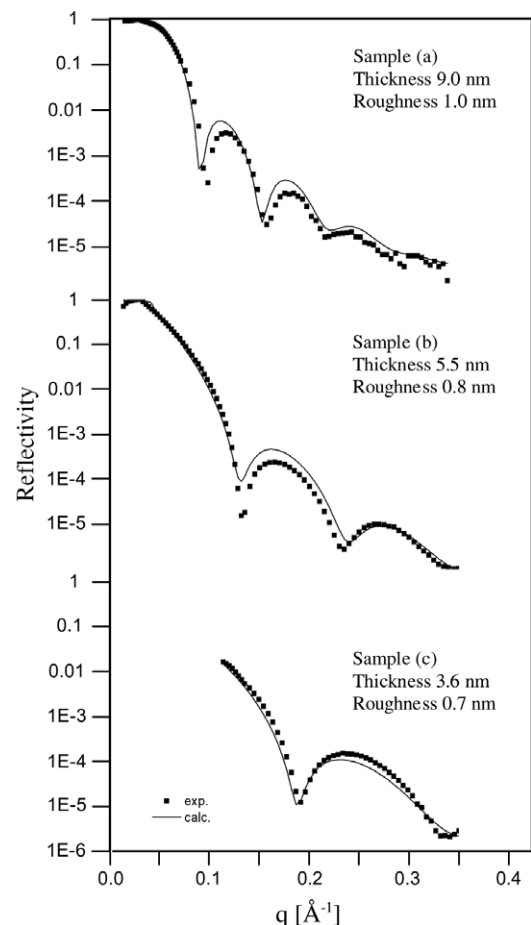


Fig. 1. Reflectivity of the Ni-films observed and calculated for three samples on sputtered Si oxide. Three different thicknesses have been used for studying the dewetting behavior on this substrate.

in situ using the procedure previously described. The lines are fit to the experimental points using a simple model based on the presence of a single, homogeneous film. The only parameters let free to vary during the fit procedure were the thickness and density of the film and the surface roughness. The interface roughness, i.e. the roughness between the substrate and the film was kept constant for all the samples because the substrates were cut from the same wafer and there was no reason to suppose a variation of this parameter across the wafer. The increase of thickness matches well the deposition time, assuming a constant flux from the evaporator. The surface roughness of the film is quite small in its absolute value and it increases slightly with the film thickness. The density of the film is about 90% of the nominal value, which is a typical result for this kind of deposition. This reduction of the film density is probably due to the presence of voids at the grain boundaries.

The dewetting is achieved by heating the sample from the deposition temperature, $T = 400$ K, in steps of 25 K, while continuously monitoring the GISAXS pattern in situ. The samples are kept at each temperature for several minutes in order to follow the occurring dynamics in real-time. During the annealing and before the dewetting

one can observe an increase in the diffuse scattering in the reflection plane, with a peak for an exit angle equal to the critical angle for X-ray reflection. Fig. 2 shows the general trend of the diffused scattering as a function of time and temperature. The images are plotted as a function of the in-plane scattering angle, $\vartheta_{//}$, and of the exit beam angle with respect to the surface, α_{out} . The formula to evaluate the scattering vector components are described elsewhere [16]. At the beginning the scattering appears only in the reflection plane. The intensity maximum is the Yoneda peak [17] which appears at the critical angle value for the outgoing beam and whose intensity depends on the surface roughness [18]. As we increase the temperature we can observe that the Yoneda peak intensity increases and its position changes going from 0.4° , the critical angle for a thick Ni-film, towards smaller exit angles. The increase of the intensity is related to an increase in the surface roughness value while the lowering of the exit angle indicates that more and more Si free surface is present. At the end (Fig. 2d) the maximum is at an exit angle of 0.32° , closer to the Si critical angle of 0.22° . The diffused intensity is concentrated in two lines symmetrically positioned around the reflectivity plane.

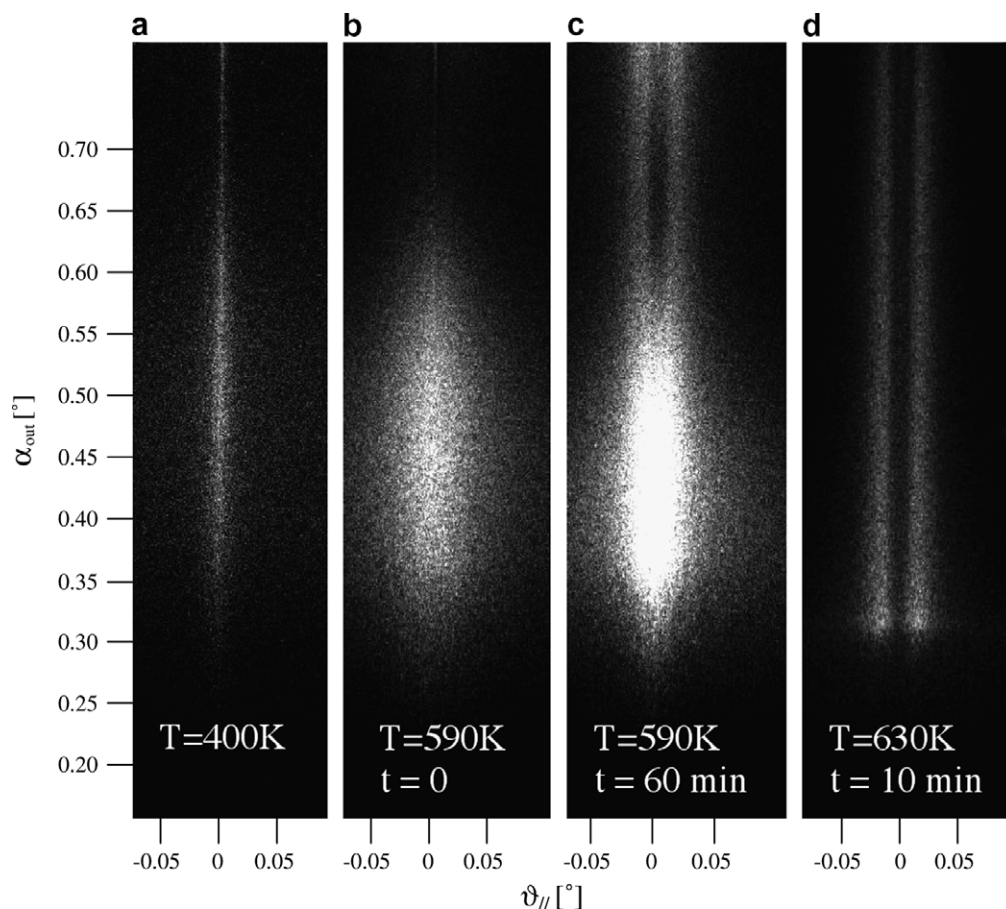


Fig. 2. GISAXS pattern during the dewetting of a Ni-film with a thickness of about 8 nm. (a) Initial state after deposition at 400 K. In (b) we show the GISAXS pattern after reaching the temperature of 590 K where the intensity of the Yoneda peak located at the Ni critical angle value of 0.4° has strongly increased. After 1 h of annealing at 590 K, intensity wings, due to the appearance of a correlation length in the roughness, appear on the sides of the reflectivity plane (c). Increasing the temperature by an additional 40 K causes the complete dewetting of the film (d). The intensity maximum occurs at a smaller exit angle of 0.325° .

The interpretation of the images corresponding to the intermediate states is difficult [19] because we do not have enough information on the surface morphology of our sample. In the final state, when the clusters are already formed, the data can be interpreted using the following relation, which is obtained in the hypothesis that the scattering intensity can be described with the same formalism used for a dense gas or a liquid [20]:

$$I(q) \propto N|F(q)|^2S(q)$$

where N is the density of the particles at the surface, $F(q)$ the particle form factor, which depends on the particles shape and dimension, and $S(q)$ is the structure factor,

which depends on the particle correlations. Because the particles have a random orientation and their dimensions follow a broad distribution, the average form factor is a slow varying function in $q_{//}$ with a maximum at $q_{//} = 0$. The scattering features are then dominated by the structure factor, which is a damped oscillatory function which goes to 1 for large $q_{//}$. Its first, and generally most intense, maxima position is related to the particle correlation average distance d , ($q_{\max, //} = 2\pi/d$) [16].

In Fig. 3, we show GISAXS patterns corresponding to the final dewetted state of the three films, which were previously characterized by X-ray reflectivity data, while in Fig. 4 we show an AFM image of the film (a) after dewett-

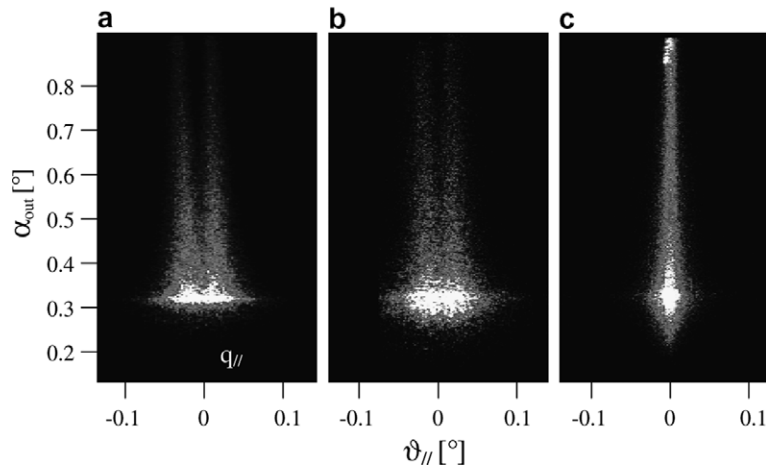


Fig. 3. GISAXS pattern after complete dewetting of Ni-films with different thicknesses: 9.0 nm in (a), 5.5 nm in (b) and 3.6 nm in (c). In this last case the dewetting was not observed.

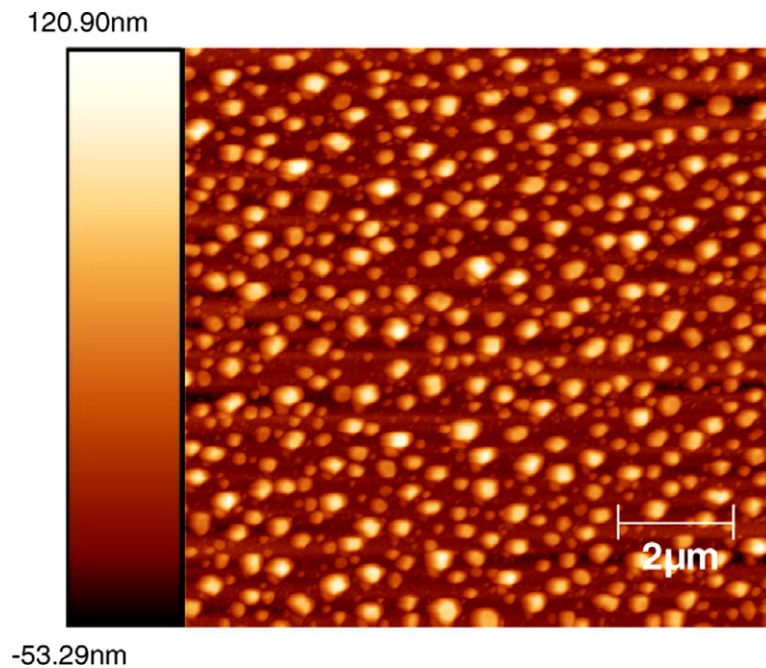


Fig. 4. Surface morphology of the sample (a) after dewetting as measured with an AFM. The surface shows the presence of well separated clusters laying on a flat substrate. The average correlation distance of the clusters, as determined by Fourier analysis of the image, is in agreement with the length determined by the GISAXS data.

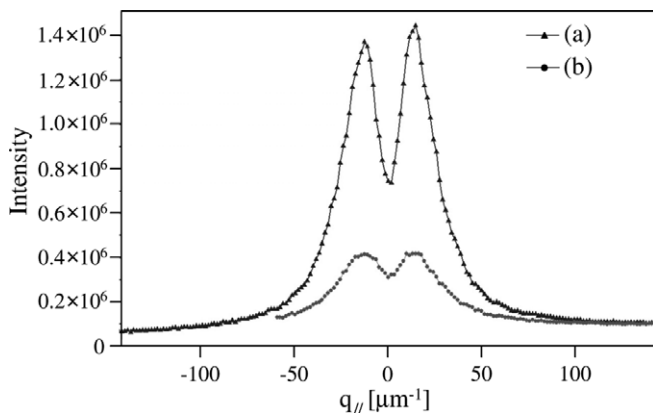


Fig. 5. Intensity cuts of the GISAXS pattern for the sample with a film thickness of 9.0 nm (a) and of 5.5 nm (b) at an exit angle of 0.32° . But data sets have their maxima at the same position of $13 \mu\text{m}^{-1}$ corresponding to a correlation length of $0.47 \mu\text{m}$.

ing illustrating the final cluster morphology of the sample. It can easily be observed that the two thicker films produced well defined intensity lines on the sides of the reflection plane. These images are characteristic for samples showing clusters while the thin one did not dewet even going up to 900 K. This implies that the thin film has a thickness smaller than a critical value and that the process occurs only for films having a thickness larger than this critical value. We must always consider that these dynamical phenomena depend on several interaction energies. Thin metal films are unstable because of their large surface/volume ratio. However in the case of films deposited onto a substrate the interaction energy between the deposited atoms and the substrate can be so strong to stabilize a thin layer, whose thickness depends on the interaction energy. The maximum thickness of the wetting layer for Ni on SiO_2 should be larger than 3.6 nm and smaller than 5.5 nm. The presence of the wetting layer in the case of the thicker films after dewetting is still an open problem.

In Fig. 5, we also report a cut of the GISAXS intensity along $q_{||}$ at an exit angle of 0.32° for samples (a) and (b). This graph shows that the position of the maxima does not depend on the film thickness. From the maxima position we can calculate a correlation length of about $0.5 \mu\text{m}$, in good agreement with the AFM image shown in Fig. 4. If the film ruptures depend on surface instabilities their characteristic wavelength should scale with the square of the film thickness [9], while if it is dominated by the grain boundaries it should go linearly [10]. Experimentally this is not the case and both mechanisms cannot be responsible for the dewetting process of thin metal solid films.

4. Conclusions

We have carried out in situ studies of the dewetting of Ni-films deposited on amorphous silicon oxide. The film

thickness and roughness have been determined using X-ray reflectometry. We have observed that dewetting leads to the formation of nano clusters for thicknesses exceeding 3.6 nm. For all the studied films we have noticed that the correlation length of the clusters does not depend on the thickness itself. This excludes both the spinodal and grain boundaries mechanisms, which were proposed to explain the phenomena. The data collected during the dewetting shows that a correlation length of the roughness appears before the dewetting of the film. This length does not vary neither with annealing time nor with film thickness and it is maintained during the whole process.

Acknowledgement

Support by the EU community under the Nano2 project, Grant No. NMP3-CT-2003-505670 is gratefully acknowledged.

References

- [1] C.A. Ross, *Annu. Rev. Mater. Res.* 31 (August) (2001) 203.
- [2] P. Tartaj, M. del Puerto Morales, S. Veintemillas-Verdaguer, T. Gonzalez-Carreno, C.J. Serna, *J. Phys. D: Appl. Phys.* 36 (2003) R182.
- [3] X. Duan, C.M. Lieber, *Adv. Mater.* 4 (2000) 298.
- [4] M. Chhowalla, K.B.K. Teo, C. Ducati, N.L. Rupesinghe, G.A.J. Amaratunga, A.C. Ferrari, D. Roy, J. Robertson, W.I. Milne, *J. Appl. Phys.* 90 (2001) 5308.
- [5] K.M. Ryu, M.Y. Kang, Y.D. Kim, H.T. Jeon, *Jpn. J. Appl. Phys., Part 1* 42 (2003) 3578.
- [6] B.L.M. Hendriksen, S.C. Bobaru, J.W.M. Frenken, *Surf. Sci.* 552 (2004) 229.
- [7] J. Bishof, D. Scherer, S. Herminghaus, P. Leiderer, *Phys. Rev. Lett.* 77 (1996) 1536.
- [8] A.L. Giermann, C.V. Thompson, *Appl. Phys. Lett.* 86 (2005) 121903.
- [9] F. Brochard Wyart, J. Daillant, *Can. J. Phys.* 68 (1990) 1084.
- [10] J.J. Rha, J.K. Park, *J. Appl. Phys.* 82 (1997) 1608.
- [11] H.C. Kim, T.L. Alford, D.R. Allee, *Appl. Phys. Lett.* 81 (2002) 4287.
- [12] R. Saxena, M.J. Frederick, G. Ramanath, W.N. Gill, J.L. Plawsky, *Phys. Rev. B* 72 (2005) 115425.
- [13] G. Renaud, R. Lazzari, C. Revenant, A. Barbier, M. Noblet, O. Ulrich, F. Leroy, J. Jupille, Y. Borensztein, C.R. Henry, J.P. Deville, F. Scheurer, J. Mane-Mane, O. Fruchart, *Science* 300 (5624) (2003) 1416.
- [14] C. Boragno, F. Buatier, G. Costantini, A. Molle, V. de Sanctis, U. Valbus, F. Borgatti, R. Felici, S. Ferrer, *Phys. Rev. B* 68 (9) (2003) 094102.
- [15] Information on the program can be found in the following HMI web address: http://www.hmi.de/bensc/instrumentation/instrumente/v6/refl/parratt_en.htm.
- [16] R. Lazzari, *J. Appl. Cryst.* 35 (2002) 406.
- [17] Y. Yoneda, *Phys. Rev.* 131 (1963) 2010.
- [18] K. Stoev, K. Sakurai, *Rigaku J.* 14 (1997) 22.
- [19] S.K. Sinha, E.B. Sirota, S. Garoff, H.B. Stanley, *Phys. Rev. B* 38 (4) (1988) 2297.
- [20] M.V. Ramana Murty, T. Curcic, A. Judy, B.H. Cooper, et al., *Phys. Rev. B* 60 (1999) 16956.